Displacement Separations by Continuous Annular Chromatography

Continuous displacement chromatography separations are obtained using a continuous annular chromatograph (CAC). The apparatus consists of a rotating annular bed. At fixed positions at the top of the bed, four solutions are continuously supplied: the feed mixture to be separated, a displacer solution, a regenerant, and a rinse. The four solutions flow concurrently through the bed with little mixing. If the bed is sufficiently deep, a fully developed displacement train forms and the separated components are continuously recovered at various angular locations at the bottom of the bed. Mixtures of amino acid were separated by cation exchange displacement chromatography in a laboratory-scale CAC. Separation and concentration of dilute mixtures was obtained with a continuous separation performance comparable with the performance of a conventional chromatograph. A mathematical model is developed to describe the separation and provide guidance in design and optimization.

Joseph P. De Carli, II
Giorgio Carta
Department of Chemical Engineering
University of Virginia
Charlottesville, VA 22903

Charles H. Byers
Chemical Technology Division
Oak Ridge National Laboratory
Oak Ridge, TN 37831

Introduction

Chromatographic separations are conventionally carried out in a batchwise fashion with fixed-bed columns. These separations, on the other hand, can be performed continuously by using a rotating annular column. In this case the apparatus, known as continuous annular chromatograph (CAC), consists of an annular bed packed in the space between two concentric cylinders. In isocratic separations, the eluent is distributed uniformly throughout the annulus at the top and flows downward. The feed mixture is supplied to a sector of the annulus that remains fixed in space while the entire bed assembly is slowly rotated on its vertical axis. With this arrangement, the feed components, having different affinities for the sorbent, travel along paths with different slopes, exiting at the bottom of the annular bed at different angular locations relative to the feed point. The elution angle in CAC operation, ϑ, is related to the elution time, t, in fixed-bed operation by

$$\vartheta = \omega t \tag{1}$$

where ω is the rate of rotation (Wankat, 1977). Thus, the least retained components will emerge closest to the feed point, while the more strongly retained components will exit at increasing angles.

The early developments of continuous annular chromatography are reviewed by Carta and Byers (1989). Recent work has focused on new applications, such as the separation of sugars (Howard, 1987; Howard et al., 1988) and the separation of proteins (Byers and Carta, 1989); on scale-up studies with pilot-scale equipment (Byers et al., 1989, 1990); and on operation with stepwise elution (Byers et al., 1988; De Carli, 1989; Carta et al., 1989). Many industrial chromatographic operations, however, are performed in displacement mode. In this case, elution of the feed mixture to the chromatographic bed is carried out with a solution containing a component (the displacer) which has affinity for the sorbent greater than that of any feed component. The displacer competes for adsorption sites desorbing and concentrating the feed components. These species will be distributed along the column length in order of decreasing affinity for the sorbent, with each upstream component acting as a "displacer" for each downstream species. The separated components exit the column as adjacent bands in order of increasing affinity. The displacer is then removed from the sorbent with an appropriate regenerant and the column conditions restored for the next feed-displacement cycle. The overall result is a separation of a dilute mixture into concentrated fractions.

Correspondence concerning this paper should be addressed to G. Carta.
Present address of J. P. De Carli, II: Dow Chemical Company, Midland, MI 48667.

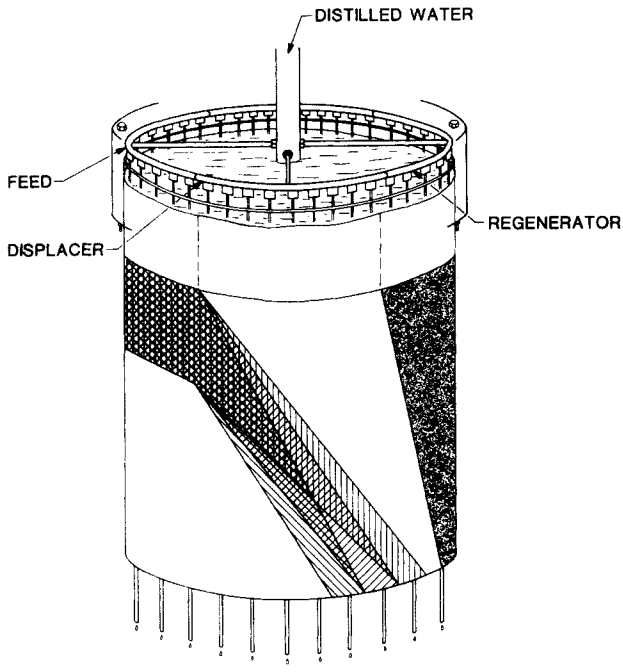

Figure 1. Continuous annular displacement chromatography apparatus.

Displacement chromatography separations can be carried out continuously with the CAC apparatus shown in Figure 1. In this case, the annular bed is provided with four different solutions: the feed to be separated, the displacer, the regenerant, and the rinse. With this arrangement, the components of a dilute feed are continuously separated in concentrated product fractions which are recovered (continuously) at fixed distances from the feed point. In this paper we provide an experimental demonstration of the use of the CAC technology for displacement chromatography separations, using mixtures of amino acids as a test system. General design guidelines and insight in the operation are obtained with a model that we have developed to predict the separation performance of the process.

Separation of Amino Acids by Ion Exchange

Ion exchange is commonly used for the separation of mixtures of amino acids. Analytical applications are broadly reported, as indicated in a typical review by Blackburn (1983). Preparative scale applications have been pioneered by Partridge and coworkers and reported in a classic series of papers (Partridge and Westfall, 1949; Partridge, 1949; Partridge and Brimley, 1949, 1951a,b, 1952; Partridge et al., 1950). Further, early work is reviewed by Saunders et al. (1989). More recent studies by Yu and Wang (1986), Yu et al. (1987), Carta et al. (1988), and Saunders et al. (1989) addressed the effects of equilibrium and mass transfer phenomena on the dynamics of fixed-bed separations of amino acids by ion exchange.

The interactions of amino acids with ion-exchange resins are complex and depend strongly on the solution pH. Amino acids are amphoteric and can be sorbed from a dilute solution by cation exchange resins at low pH and by anion exchange resins at high pH. Displacement separations can be carried out with either resin type. Using a cation exchange resin bed, for example, a strong base is used as the displacer. At high pH, the amino acids become negatively charged and are excluded from the resin moving downstream of the displacer front that propagates through the column. Downstream of this front, the solution composition is determined by the competitive multicomponent sorption behavior of the amino acids. This, in turn, is dependent on the ionization constants of the amino acids and the specific affinities of the individual amino acid cations for the resins' functional groups.

Equipment and Experimental Methods

Materials

The resin used in this study is Dowex 50W-X8, a sulfonated, polystyrene-divinylbenzene resin with a nominal degree of crosslinking of 8%. A commercial resin sample was elutriated to recover a fraction in the 37–55 μm particle size range. The total ion-exchange capacity of the resin is 5.6 ± 0.2 mmol/g dry resin and the dry weight of the hydrogen form of the resin is 0.45 ± 0.04 g dry resin/g wet resin (Dye et al., 1989).

A mixture of L-glutamic acid, L-valine, and L-leucine was selected as a model separation system. Relevant physicochemical properties of these compounds are given in Table 1. The three amino acids were obtained with purity greater than 99% from Ajinomoto USA, Inc. and Sigma Chemical, and were used without further purification. Other chemicals were obtained from Fisher and were analytical reagent grade. The concentrations of amino acids in aqueous solutions were determined by HPLC using the technique described by Dye (1988).

Equipment

Both fixed-bed and CAC experiments were carried out to provide a comparison of performance. For fixed-bed experiments, the resin was packed in a glass column 1.5 cm in diameter (Spectrum Scientific) to a height of 20 cm. The feed solutions were prepared by dissolving the amino acids in deionized distilled water and loaded onto the column with a Waters 501 HPLC pump. The displacer, a NaOH solution, was fed directly

Table 1. Equilibrium Parameters, $t = 25°C$

Amino Acid	Solubility* (mM)	pK_1^{**}	pK_2^{**}	pK_3^{**}	pI	$\bar{S}$†
L-Glu	58.7	2.19	4.25	9.67	3.22	1.0
L-Val	755	2.32	9.62	—	5.97	1.0
L-Leu	184	2.36	9.62	—	5.99	3.0

*Weast (1977)
**Meister (1965)
†Dye et al. (1990)

after the amino acids. Samples of the effluent were collected with a Gilson Model 231 fraction collector.

The CAC apparatus was constructed of Plexiglas and is similar to the one described by Howard et al. (1988). The annulus is formed between two concentric cylinders flanged at the bottom, and is 27.9 cm in outside diameter with a width of 1.27 cm. A head space is left at the top for the introduction of feed and eluents. The Dowex resin, slurry packed in the annulus to a height of 22 cm, is supported at the bottom by porous polyethylene plugs. A 10 cm layer of glass beads, 0.045 cm in diameter, was packed on top of the resin bed to prevent convective mixing of the eluents and provide uniform flow distribution. The effluent flows through a set of 180 stainless steel tubes attached at the bottom of the bed. The entire assembly is rotated by a shaft connected to the bottom flange around a stationary inlet distributor that passes through the top flange.

The feed, displacer, and regenerant (50 m*M* sulfuric acid) are supplied by positive displacement pumps (Milroyal Mod DC-1-175R) and distributed through headers to a system of nozzles uniformly spaced 7.5 degrees apart. The nozzles were constructed of 0.159 cm stainless steel tubing, 300 μm in inside diameter. The individual nozzles in each header, approximately 6.5 cm long, were matched to provide essentially the same flow for a pressure drop of 0.28 kPa. The tips of these nozzles penetrated approximately 6.0 cm into the glass bead layer. The rinse solution (deionized distilled water) was supplied directly to the top of the CAC unit and filled the entire head space, flowing in the sector of annulus not occupied by the other three solutions. Tracer experiments, using blue dextran 2000 (Pharmacia) as a visible dye, revealed that uniform flow distribution without mixing or fingering could be obtained. Since the pressure drop through the unit is the same throughout the annulus and the permeability of the packed resin bed is essentially uniform, the fluid superficial velocity is constant. Thus, each of the solutions, being fed at a constant rate, occupies a sector of the annulus proportional to its flow rate. The spacing of the nozzles is such that a continuous band is formed for each sector and the rinse solution flows only in the sector not occupied by nozzles.

To monitor the operation of the apparatus, a peristaltic pump was used to continuously withdraw a steady fluid stream from one of the exit tubes at a rate equal to 1/180 of the total flow through the bed. Fractions collected from this stream were then analyzed to determine the effluent concentration profile.

Theoretical Development

Isotachic concentrations

Modeling the chromatographic separation of amino acids with a cation exchange resin bed requires a knowledge of the solution dissociation equilibria of the amino acids as well as of the specific interactions of the amino acid cations with the resins' functional groups. Being amphoteric, amino acids tend to buffer the solution in which they are present at their isoelectric pH. In the absence of a dominant buffer, therefore, the solution pH of a mixture of amino acids is determined by the composition of the mixture itself.

The equilibrium uptake of glutamic acid, valine, and leucine by the hydrogen form of Dowex 50W-X8 has been determined by Dye et al. (1990). The experimental pure-component uptake of the three amino acids in pure water is shown in Figure 2. The

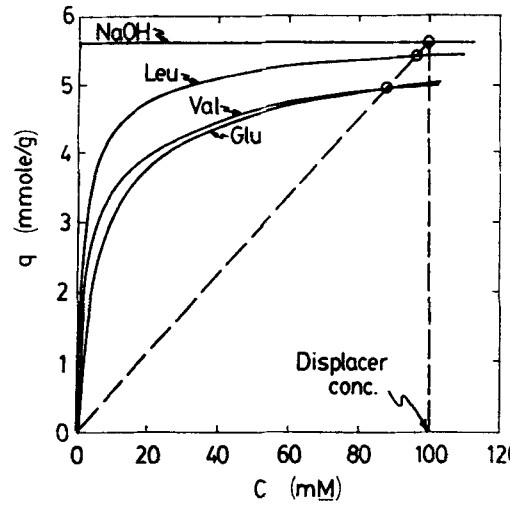

Figure 2. Isotachic concentrations for a displacer concentration of 100 m*M*.

Solid lines are the pure-component uptake curves.

equilibrium uptake of sodium ion from NaOH solutions is also shown in this figure. Since the resin is strongly acidic, the latter curve is essentially rectangular. The maximum product concentrations achievable in the displacement chromatography of these amino acids using NaOH as the displacer may be easily predicted from these data (Glueckauf, 1949; Helfferich and Klein, 1970). If the column is sufficiently long, the displaced components achieve constant velocity or "isotachic" concentrations that are determined from a solution of the equations

$$v_c^{Na} = v_c^{GLU} = v_c^{VAL} = v_c^{LEU}, \tag{2}$$

or

$$\frac{\Delta q_{Na}}{\Delta C_{Na}} = \frac{\Delta q_{GLU}}{\Delta C_{GLU}} = \frac{\Delta q_{VAL}}{\Delta C_{VAL}} = \frac{\Delta q_{LEU}}{\Delta C_{LEU}}, \tag{3}$$

where Δ indicates the difference between concentration values downstream and upstream of the displacement front. A graphical interpretation of the procedure is shown in Figure 2. The chord drawn between the initial NaOH concentration in the bed (0 m*M*) and the point on the displacer equilibrium curve corresponding to the displacer feed concentration (100 m*M* in this example) intersects the amino acid equilibrium curves at their isotachic concentrations. Although valine and glutamic acid have essentially the same pure component uptake curve at their respective isoelectric pH, their separation is possible as a result of differences in their isoelectric pH values. At the pI of valine (~6), in fact, glutamic acid (pI ~ 3.2), is negatively charged and moves faster down the column to be reabsorbed downstream of the valine band. The separated components will thus exit in order of increasing pI. Leucine will be the last species to exit the column before the displacer as a result of its higher pI and affinity for the resin.

In view of the analogy expressed by Eq. 1, the same procedure provides the maximum achievable product concentrations in CAC operation. The angular concentration velocity of a species

i becomes simply expressed by

$$\left(\frac{dz}{d\vartheta}\right)_i = \frac{v_c^i}{\omega} \tag{4}$$

Equilibrium stage model

Models for displacement chromatography operations have been recently reviewed by Cramer and Subramanian (1989). In our case, the experimental system contains: five exchangeable counterions—three amino acid cations (glutamic acid, valine, and leucine), sodium and hydrogen ions; and five coions—three amino acid anions, hydroxyl ion, and sulfate ion. In addition, the zwitterionic forms of the three amino acids will also be present. As shown by Carta et al. (1988) and Saunders et al. (1989), it is convenient to write the material balances for the total concentrations, C_{A_i}, of the three amino acids and for sodium. The local pH and the concentrations of the cationic, anionic and zwitterionic forms can then be calculated from the electroneutrality condition. An additional material balance is needed for the sulfate coion if this is present and variable.

Considering a fixed-bed displacement operation (the steady-state behavior of the CAC may be immediately obtained from this development via the transformation expressed by Eq. 1) and focusing on the feed-loading and displacement steps, the following continuity equations can be written

$$\epsilon\frac{\partial C_{A_1}}{\partial t} + \rho_b\frac{\partial q_{A_1}}{\partial t} + u\frac{\partial C_{A_1}}{\partial z} = 0 \tag{5}$$

$$\epsilon\frac{\partial C_{A_2}}{\partial t} + \rho_b\frac{\partial q_{A_2}}{\partial t} + u\frac{\partial C_{A_2}}{\partial z} = 0 \tag{6}$$

$$\epsilon\frac{\partial C_{A_3}}{\partial t} + \rho_b\frac{\partial q_{A_3}}{\partial t} + u\frac{\partial C_{A_3}}{\partial z} = 0 \tag{7}$$

$$\epsilon\frac{\partial C_{Na^+}}{\partial t} + \rho_b\frac{\partial q_{Na}}{\partial t} + u\frac{\partial C_{Na^+}}{\partial z} = 0 \tag{8}$$

with the initial and boundary conditions

$$t = 0,\ z > 0: \qquad q_{A_i} = q_{Na} = C_{A_i} = C_{Na^+} = 0$$

$$z = 0,\ 0 < t \le t_F: \quad C_{A_i} = C_{A_i}^F,\ C_{Na^+} = 0$$

$$t > t_F: \qquad C_{A_i} = 0,\ C_{Na^+} = C_{Na^+}^D$$

where the $C_{A_i}^F$'s are the feed concentrations of the amino acids, and $C_{Na^+}^D$ is the displacer concentration. To simplify the numerical calculations, we neglect the rates of accumulation of solutes in the interstitial liquid space. Since the resin capacity is quite high, this approximation results in an error of less than 6% in the prediction of the breakthrough time of the displacer front. The first term in Eqs. 5–8, therefore, can be discarded. The partial differential equations are discretized by using backward differences following the procedure used by Friday and LeVan (1982). After minor rearrangement, Eqs. 5–8 yield,

$$\frac{dq_{A_1}^j}{dt} = \frac{u}{\rho_b\Delta z}\left(C_{A_1}^{j-1} - C_{A_1}^j\right) \tag{9}$$

$$\frac{dq_{A_2}^j}{dt} = \frac{u}{\rho_b\Delta z}\left(C_{A_2}^{j-1} - C_{A_2}^j\right) \tag{10}$$

$$\frac{dq_{A_3}^j}{dt} = \frac{u}{\rho_b\Delta z}\left(C_{A_3}^{j-1} - C_{A_3}^j\right) \tag{11}$$

$$\frac{dq_{Na}^j}{dt} = \frac{u}{\rho_b\Delta z}\left(C_{Na^+}^{j-1} - C_{Na^+}^j\right) \tag{12}$$

The procedure is equivalent to modeling the bed as if it were composed of a series of equilibrium stages. At each stage, j, the fluid concentration C_i^j is at any time in equilibrium with the resin solute concentration q_i^j. Hydrodynamic dispersion and mass transfer resistances are not explicitly accounted for in the formulation of the model. They are, however, introduced in an approximate manner by the numerical dispersion caused by the finite difference approach used for the solution of the model equations (Lin et al., 1989).

Method of solution

To solve these equations it is necessary to have a description of the uptake equilibrium on the resin. Dye et al. (1990) have expressed the multicomponent uptake of amino acids as a function of the ionic fractions of amino acid cations and hydrogen ions as

$$Y_{A_i} = \frac{q_{A_i}}{q_o} = \frac{S_i X_{A_i}}{X_H + \sum_i S_i X_{A_i}} \tag{13}$$

where q_o is the ion-exchange capacity of the resin. The S_i values are the selectivity coefficients for the exchange of amino acid cation i with hydrogen ion. The ionic fractions X_{A_i} are given by

$$X_{A_i} = \frac{C_{A_i^+}}{C_{H^+} + \sum_k C_{A_k^+}} \tag{14}$$

The total "analytical" concentration of each of the three amino acids, C_{A_i}, is equal to the sum of all its ionic forms and can be calculated from

$$C_{A_i} = C_{A_i^+} + C_{A_i^\pm} + C_{A_i^-} + C_{A_i^{=}} \tag{15}$$

where for each amino acid

$$C_{A_i^+} = C_{A_i}\left/\left(1 + \frac{K_{1_i}}{C_{H^+}} + \frac{K_{1_i}K_{2_i}}{C_{H^+}^2} + \frac{K_{1_i}K_{2_i}K_{3_i}}{C_{H^+}^3}\right)\right. \tag{16}$$

$$C_{A_i^-} = C_{A_i}\left/\left(1 + \frac{C_{H^+}}{K_{2_i}} + \frac{C_{H^+}^2}{K_{1_i}K_{2_i}} + \frac{K_{3_i}}{C_{H^+}}\right)\right. \tag{17}$$

$$C_{A_i^{=}} = C_{A_i}\left/\left(1 + \frac{C_{H^+}}{K_{3_i}} + \frac{C_{H^+}^2}{K_{2_i}K_{3_i}} + \frac{C_{H^+}^3}{K_{1_i}K_{2_i}K_{3_i}}\right)\right. \tag{18}$$

Here K_{1_i}, K_{2_i}, and K_{3i} are the dissociation constants of the amino acids. For valine and leucine, K_3 and $C_{A^=}$ are zero. Finally, the

electroneutrality condition is expressed by

$$\sum_i C_{A_i^-} + C_{Na^+} + C_{H^+} = \sum_i C_{A_i^-} + K_W/C_{H^+} + 2\sum_i C_{A_i^-} \quad (19)$$

where K_W is the ionic product of water.

For efficient computation, fluid-phase compositions, C_i, should be known explicitly as a function of the resin composition, q_i. To simplify the calculations, we assumed that the binary selectivities, S_i, are constants equal to their mean values, $\overline{S}_i$, defined by Dye et al. (1990), which are given for the three amino acids in Table 1. Using these constant selectivity values results in an error of ~10% in the evaluation of the maximum uptake capacity. This assumption allows inversion of Eq. 13 yielding

$$X_{A_i} = \frac{Y_{A_i}/\overline{S}_i}{Y_H + \sum_i Y_{A_i}/\overline{S}_i} \quad (20)$$

Finally, we make the assumption that, because of the irreversible nature of the uptake of sodium from NaOH solutions, the displacer front is sharp. The assumption is reasonable for even a few equilibrium stages, since the equilibrium so strongly favors desorption of the amino acids from the resin at high pH. As a result, no amino acids are present upstream of the high pH front where the resin is completely in the sodium form ($q_{Na} = q_o$); downstream of the front no sodium is present. The front moves at a velocity which is approximately given by

$$v_c^{Na} = u\Big/\left(\rho_b \frac{q_o}{C_{Na}^D}\right) \quad (21)$$

Equations 9–11 need to be integrated downstream of the displacement front to obtain the local composition. The procedure for integrating these equations over one time step is straightforward, given the current values of $C_{A_i}^j$ at each stage and $C_{A_i}^{j-1}$ for the feed stage. This yields new q_i^j values for each stage which are used in Eq. 20 to compute $X_{A_i}^j$ and X_H^j. The latter values are then used in conjunction with Eqs. 16–19 to compute the total concentration of counterions ($=C_{H^+} + \Sigma_k C_{A_k^+}$) which permits the computation of the concentrations of cationic, anionic and zwitterionic forms of the amino acids. (This amounts to the solution of a cubic equation derived from Eq. 19.) Finally, the total analytical concentrations of the individual amino acids, $C_{A_i}^j$ are computed for each stage from Eq. 15, and the integration is continued with these new values. The Adams predictor-corrector method was used for the integration, and the number of stages, N, was used as an adjustable parameter to attain a fit to experimental concentration profiles.

Results and Discussion

Fixed-bed operation

Figure 3 shows the experimental product concentration and pH histories for the displacement chromatography in a fixed bed of a mixture containing 15.4 mM glutamic acid, 15.0 mM valine, and 16.2 mM leucine. In this experiment the feed was

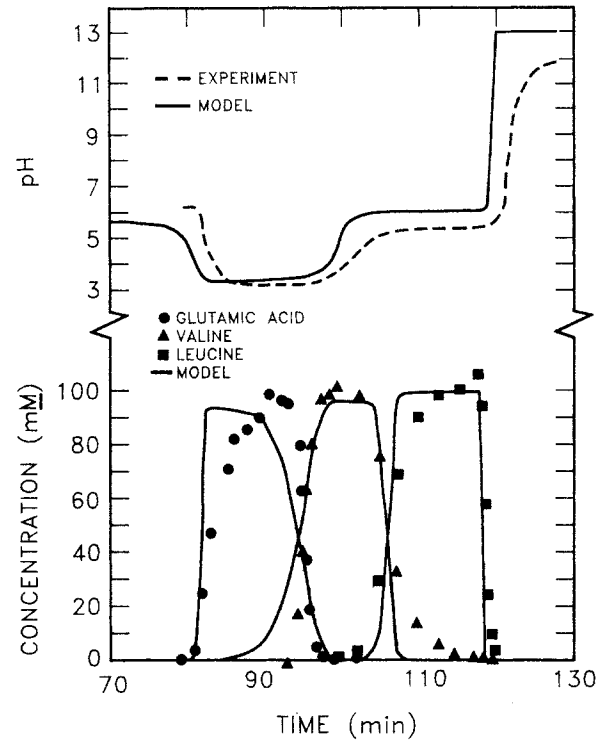

Figure 3. Experimental and calculated product concentration and pH histories for displacement separation in a fixed bed.

supplied to the bed for 75 min, the displacer concentration was 100 mM, and the superficial velocity was 3.1 cm/min. The order of elution is in agreement with the batch equilibrium measurements and the peak concentrations are consistent with the isotachic concentrations determined by the method in Figure 2. The experimental pH profile closely reflects the separation resulting from the buffering effect of the amino acids. Initially the pH is ~7 and reaches a plateau at about 3 when glutamic acid is eluted. The pH then rises to values between 5 and 6 during the elution of valine and leucine, and makes a final jump to a value between 12 and 13 when the NaOH front breaks through. Glutamic acid was eluted at concentrations which exceeded its solubility limit in water; and while the eluted fractions were initially clear, a precipitate was formed after a few days.

Calculated profiles based on the equilibrium stage model with $N = 50$ are also shown in Figure 3. The bed density, $\rho_b = 0.33$ g dry resin/cm^3 bed, was obtained by draining the bed and drying its contents, and the bed void fraction, $\epsilon = 0.40$, was determined from the retention time of a pulse of blue dextran. Because the fluid-phase accumulation was neglected, the model slightly underestimated the breakthrough of NaOH. To correct for this deviation, the entire calculated profile was shifted in time by adding the quantity $\epsilon z/u$. With this correction, amounting to approximately 3% of the NaOH breakthrough time, calculated and experimental chromatograms were in good agreement. The leading and trailing edges of the peaks indicate the areas of most significant variance between experiment and theory. These portions of the curves are most seriously affected by the exact shape of the uptake equilibrium curves and by mass transfer

Table 2. Base Conditions for CAC Operation

Feed conc.*	25 m*M*	Glu
	25 m*M*	Val
	25 m*M*	Leu
Displacer conc.	100 m*M*	NaOH
Regenerant conc.	50 m*M*	H_2SO_4
Feed sector	45	deg
Displacer sector	90	deg
Regenerant sector	90–180	deg
Bed length	22	cm
Rotation rate	30	deg/h
Superficial velocity	2.9	cm/min

*In deionized distilled water

resistances. Therefore, the assumption of constant ion-exchange selectivities and the quantitative modeling of mass transfer resistance by the finite number of stages are likely to be responsible for such discrepancies.

Sharp trailing edges in the leucine experimental profiles are predicted by the equilibrium stage model. Because of the rectangular character of the NaOH uptake curve, the model predicts an essentially vertical line, even with a single stage. Therefore, dispersion of the leucine-NaOH boundary, which is due almost exclusively to mass transfer resistances (Carta et al., 1989), is not described by the model.

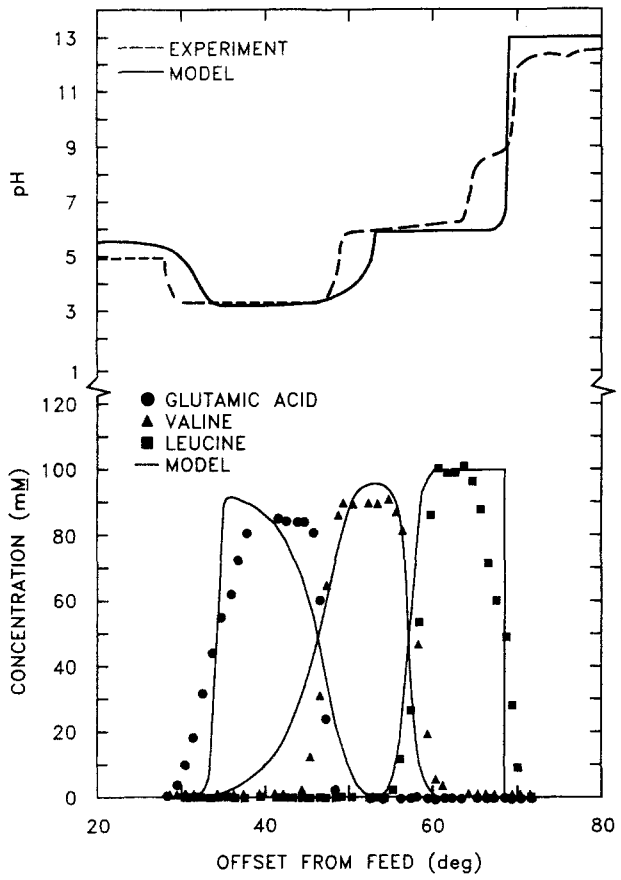

Figure 4. Experimental and calculated product concentration and pH profiles for continuous displacement separation in CAC at base conditions (Table 2).

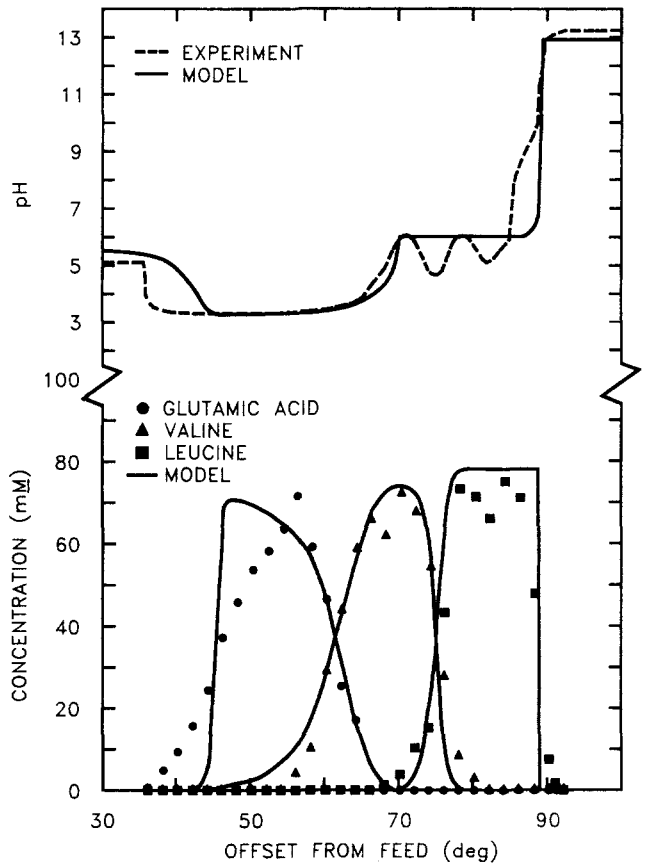

Figure 5. Experimental and calculated product concentration and pH profiles for continuous displacement separation in CAC with a displacer concentration of 80 m*M*.

CAC operation

The operating conditions of the CAC apparatus are listed in Table 2, and an experimental CAC chromatogram is shown in Figure 4. The origin of the angular coordinate is set at the boundary between the feed sector and the displacement sector and only the amino acid profiles are shown. The resin was completely converted to the hydrogen form in the regeneration sector of the CAC. Although the feed concentrations were different, a qualitative comparison can be made between this run and the fixed-bed separation in Figure 3, since the fluid velocity, the bed length, and the displacer concentration were nearly the same. The quality of the separation is comparable, and the plateau concentrations are nearly the same. The CAC plateaus, however, are wider. The leucine plateau, for example, has a duration of approximately 12 min in the fixed bed. At a rotation rate of 30 deg/h this corresponds to a 6 deg sector in CAC operation (Eq. 1). The experimental leucine peak occupies approximately a 10 deg sector, which is in the same proportion to the 6 deg sector as the ratio of feed concentrations in the two runs. Calculated concentration and pH profiles based on the equilibrium stage model with $N = 50$ are shown in Figure 4. The general agreement between experimental and calculated profiles is essentially the same as that observed for the fixed-bed run, revealing that the CAC provides little or no additional peak dispersion relative to a corresponding conventional chromatography process.

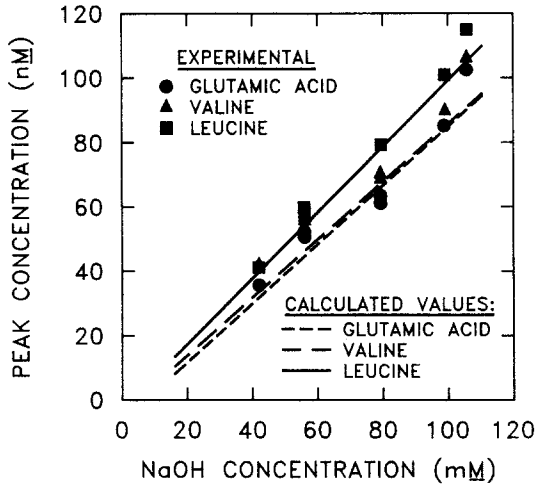

Figure 6. Experimental and calculated effects of displacer concentration on peak product concentrations.

Figure 5 shows experimental and calculated concentration and pH profiles using a displacer concentration of 80 mM, and Figure 6 shows the experimental peak (maximum) concentrations obtained with different NaOH concentrations in comparison with the isotachic concentrations predicted by the method illustrated in Figure 2. At NaOH concentrations above 40 mM, the product concentrations become directly proportional to the displacer concentration. As is evident from Figure 2, this occurs because the uptake curves of the three amino acids level out to nearly constant at concentrations above 40 mM.

The concentration and pH profiles for a CAC run with an amino acid feed concentration of 10 mM are shown in Figure 7. For the purpose of a qualitative comparison, 50 stages were used again for the model calculations since the hydrodynamics was identical to the other runs in the series. Obviously, a smaller number of stages would have provided a better quantitative agreement. The peak concentrations are now considerably lower than the isotachic values, and the plateaus are largely eroded by dispersion and mass transfer resistances. For such a dilute feed, a wider feed sector (and feed flow rate) would have been needed to achieve the isotachic concentrations. The experimental and calculated peak concentrations obtained at different feed concentrations are shown in Figure 8. For feed concentrations above approximately 15 mM (but below the displacer concentration), the amino acid loading permits the achievement of isotachic concentrations. Below this value, the product decreases rapidly.

The effects of rotation rate on the peak concentrations are shown in Figure 9. These effects are important as decreasing the rotation rate increases the feed loading and thus the capacity of the apparatus. Isotachic concentrations are achieved for all components at 15 deg/h. Above this value, the peak concentrations remain constant while the resin loading with feed per unit cross sectional area of the bed, Q, decreases according to the equation

$$Q = \frac{C^F u Q_F}{Q_T} \frac{360°}{\omega} \tag{22}$$

where C^F and Q_F are the feed concentration and flow rate, and Q_T the total flow rate. As a consequence, the feed throughput allowed for the unit decreases as the displacement train exits at a large offset from the feed sector. If the rotation rate is too low, on the other hand, the displacement train may not be fully

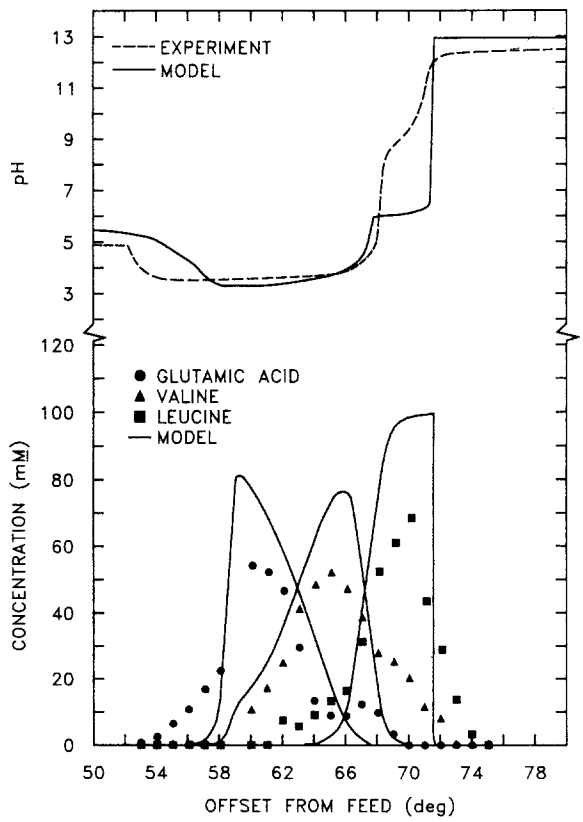

Figure 7. Experimental and calculated product concentration and pH profiles for continuous displacement separation in CAC with a feed concentration of 10 mM for each amino acid.

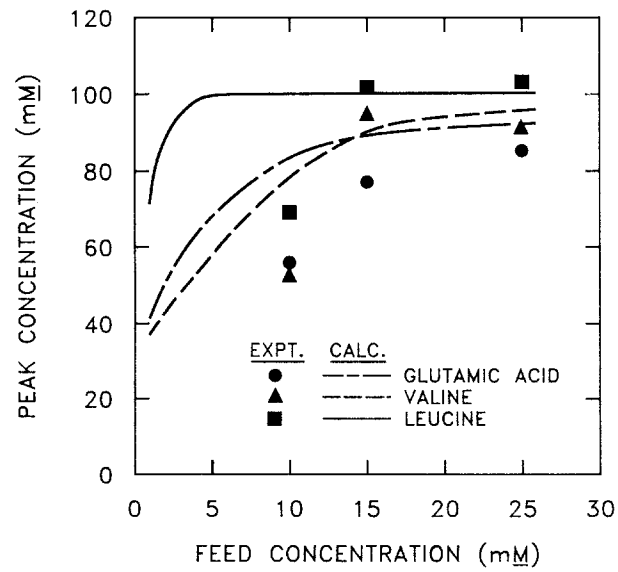

Figure 8. Experimental and calculated effects of feed concentration on peak product concentrations.

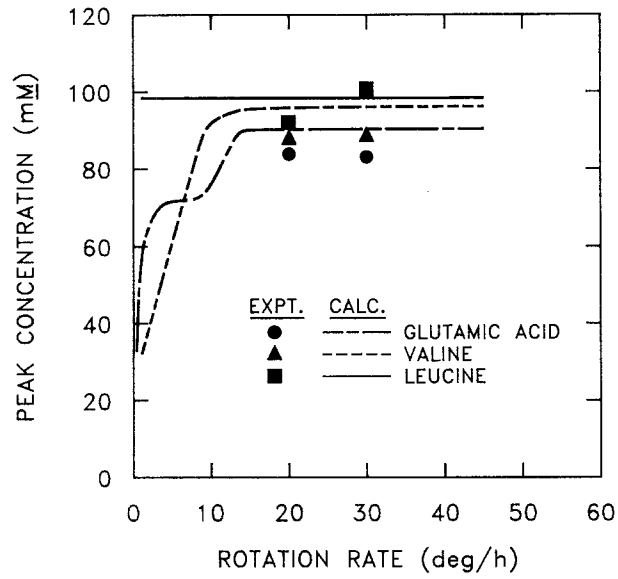

Figure 9. Experimental and calculated effects of rotation rate on peak product concentrations.

formed and some of the amino acids may exit the column before having interacted with the displacer. As an example, calculated concentration and pH profiles at 10 deg/h are shown in Figure 10. The leucine profile reaches isotachic condition and exhibits a plateau. The profiles for glutamic acid and valine, however, are more complicated, exhibiting three plateaus and a low degree of separation. The leading glutamic acid plateau and the gradual rising of valine from zero to about 40 mM result from the competitive adsorption of glutamic acid, valine, and leucine during loading of the feed onto the hydrogen form of the resin. The remaining transitions are caused by the interference with the displacer. Had the bed been deeper, the displacer wave would have overtaken the noncoherent transitions displayed here for glutamic acid and valine forming a fully resolved displacement train.

Concluding Remarks

We have demonstrated the operation of a continuous annular chromatograph for the separation of dilute mixtures of amino acids by displacement development using a cation-exchange resin. The technique allows simultaneous separation and concentration of multicomponent mixtures to be performed in a continuous, steady-state fashion. The separation quality obtained with a laboratory-scale CAC apparatus was compared with that generated with a comparable fixed-bed chromatograph. It appears that even in displacement development mode of operation, the continuous performance of the CAC is very nearly the same as the batchwise performance of the corresponding fixed-bed process.

In this work we developed a useful mathematical model that describes the fundamental features of the system. Details of the equilibrium relationship and the individual-component mass transfer could be added at the expense of considerable computer time. On the other hand, our relatively simple model allows an approximate prediction of the concentration levels and of the separatiin performance achievable requiring only equilibrium data.

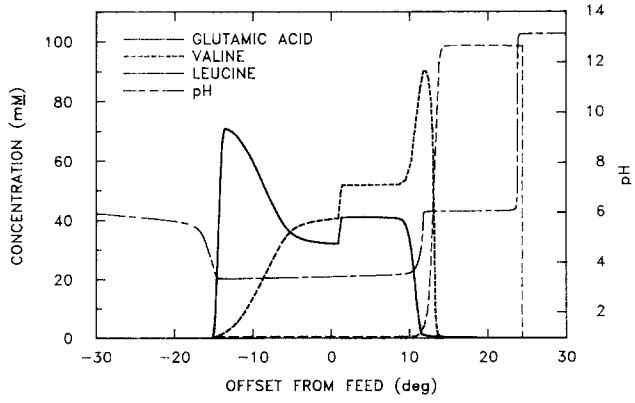

Figure 10. Calculated product concentration and pH profiles for continuous displacement separation in CAC with a rotation rate of 10 deg/h.

Acknowledgment

This research was sponsored in part by the Office of Industrial Programs, U.S. Department of Energy, under Contract DE-AC05-84OR21400 with Martin Marietta Energy Systems, Inc., by the Virginia Center for Innovative Technology, and by National Science Foundation Grant CBT-8709011.

Notation

C_i = liquid-phase solute concentration, g/L
K_W = ionic product of water, mol^2/L^2
K_{1i} = first dissociation equilibrium constant, mol/L
K_{2i} = second dissociation equilibrium constant, mol/L
K_{3i} = third dissociation equilibrium constant, mol/L
N = number of equilibrium stages
q_i = resin solute concentration, mmol/g dry resin
q_o = resin ion-exchange capacity, mmol/g dry resin
Q = resin loading with feed per unit bed cross sectional area, mmol/cm^2
Q_F = feed flow rate, cm^3/s
Q_T = total flow rate, cm^3/s
S_i = binary ion-exchange selectivity for cation i relative to hydrogen ion
$\overline{S}_i$ = mean binary ion-exchange selectivity for cation i relative to hydrogen ion
t = time, s
u = superficial velocity, cm/s
v_c^i = concentration velocity, cm/s
X_i = liquid phase ionic fraction of cation i
Y_i = resin phase ionic fraction of cation i
z = bed axial position, cm

Greek letters

ϵ = bed void fraction
ϑ = angular coordinate: offset from feed, deg
ρ_b = bed density, g dry resin/cm^3
ω = rotation rate, deg/s

Superscripts

D = displacer value
F = feed value

Literature Cited

Blackburn, S., "Amino Acids and Amines," *Handbook of Chromatography*, G. Zŵeig and J. Sherma, eds., CRC Press, Boca Raton, FL (1983).

Byers, C. H., W. G. Sisson, and J. P. DeCarli, II, "The Use of Gradient Elution in Optimizing Continuous Annular Ion Exchange Chromatog-

raphy with Application to Metal Separations," *Ion Exchange for Industry*, Michael Streat, ed., Ellis Harwood, Chichester, 242 (1988).
Byers, C. H., W. G. Sisson, J. P. DeCarli, II, and G. Carta, "Pilot-Scale Studies of Sugar Separations by Continuous Chromatography," *Appl. Biochem. Biotech.*, **20,** 635 (1989).
———, "Sugar Separations on a Pilot Scale by Continuous Annular Chromatography," *Biotech. Prog.*, **6,** 13 (1990).
Byers, C. H., and G. Carta, "Application of Continuous Annular Chromatography to Biochemical Separations," *Symp. on Separation Science for Energy Applications*, Knoxville, TN (1989).
Carta, G., and C. H. Byers, "Novel Applications of Continuous Annular Chromatography," *New Directions in Sorption Technology*, G. E. Keller and R. T. Yang, eds., Butterworth, Stoneham (1989).
Carta, G., J. P. DeCarli, II, C. H. Byers, and W. G. Sisson, "Separation of Metals by Continuous Annular Chromatography with Step Elution," *Chem. Eng. Commun.* **79,** 207 (1989).
Carta, G., M. S. Saunders, J. P. DeCarli, II, and J. B. Vierow, "Dynamics of Fixed-Bed Separations of Amino Acids by Ion-Exchange," *AIChE Symp. Ser.* **84,** 54 (1988).
Carta, G., M. S. Saunders, and F. Mawengkang, "Studies on the Diffusion of Amino Acids in Cation Exchange Resins," *Int. Conf. on Fundamentals of Adsorption*, Sonthöfen, West Germany (1989).
Cramer, S. M., and G. Subramanian, "Preparative Chromatography of Biomolecules—New Directions," *New Directions in Sorption Technology*, G. E. Keller and R. T. Yang, eds., Butterworth, Stoneham (1989).
DeCarli, II, J. P., "Improved Operation and Novel Applications of Continuous Annular Chromatography," PhD Diss., Univ. of Virginia, Charlottesville (1989).
Dye, S. R., "Equilibrium Uptake of Amino Acids by a Strong-Acid Cation Exchange Resin," Undergraduate Thesis, Univ. of Virginia, Charlottesville (1988).
Dye, S. R., J. P. DeCarli, II, and G. Carta, "Equilibrium Sorption of Amino Acids by a Cation Exchange Resin," *Ind. Eng. Chem. Res.*, **29,** 849 (1990).
Friday, D. K., and M. D. LeVan, "Solute Condensation in Adsorption Beds During Thermal Regeneration," *AIChE J.*, **28,** 86 (1982).
Glueckauf, E., "Theory of Chromatography: VII. General Theory of Two Solutes Following Nonlinear Isotherms," *Discuss. Farad. Soc.*, **7,** 12 (1949).
Helfferich, F., and G. Klein, *Multicomponent Chromatography*, Marcel Dekker, New York (1970).
Howard, A. J., "Separation of Sugars by Continuous Annular Chromatography," MS Thesis, Univ. of Virginia, Charlottesville (1987).
Howard, A. J., G. Carta G., and C. H. Byers, "Separation of Sugars by Continuous Annular Chromatography," *Ind. Eng. Chem. Res.*, **27,** 1873 (1988).
Lin, B., Z. Ma, and G. Guiochon, "Influence of Calculation Errors in the Numerical Simulation of Chromatographic Elution Band Profiles using an Ideal or Semiideal Model," *J. Chromatogr.*, **484,** 83 (1989).
Meister, A., *Biochemistry of the Amino Acids*, Vol. I, Academic Press, New York (1965).
Partridge, S. M., "Displacement Chromatography on Synthetic Ion-Exchange Resins: 3. Fractionation of a Protein Hydrolysate," *Biochem.*, **44,** 521 (1949).
Partridge, S. M., and R. C. Brimley, "Displacement Chromatography on Synthetic Ion-Exchange Resins: 6. Effect of Temperature on the Order of Displacement," *Biochem.*, **48,** 313 (1951a).
———, "Displacement Chromatography on Synthetic Ion-Exchange Resins: 2. The Separation of Organic Acids and Acidic Amino Acids by the Use of Anion-Exchange Resins," *Biochem.*, **44,** 513 (1949).
———, "Displacement Chromatography on Synthetic Ion-Exchange Resins: 7. Separations Using a Strongly Basic Resin," *Biochem.*, **49,** 153 (1951b).
———, "Displacement Chromatography on Synthetic Ion-Exchange Resins: 8. A Systematic Method for the separation of Amino Acids," *Biochem.*, **51,** 628 (1952).
Partridge, S. M., R. C. Brimley, and K. W. Pepper, "Displacement Chromatography on Synthetic Ion-Exchange Resins: 5. Separation of the Basic Amino Acids," *Biochem.*, **46,** 334 (1950).
Partridge, S. M., and R. G. Westfall, "Displacement Chromatography on Synthetic Ion-Exchange Resins: 1. Separation of Organic Bases and Amino Acids," *Biochem.*, **44,** 418 (1949).
Saunders, M. S., J. B. Vierow, and G. Carta, "Uptake of Phenylalanine and Tyrosine by a Strong-Acid Cation Exchanger," *AIChE J.*, **35,** 53 (1989).
Wankat, P. C., "The Relationship between One Dimensional and Two Dimensional Separation Processes," *AIChE J.*, **23,** 859 (1977).
Weast, R. C., *Handbook of Chemistry and Physics*, CRC Press, Boca Raton, FL (1977).
Yu, Q., and N.-H. L. Wang, "Multicomponent Interference Phenomena in Ion Exchange Columns," *Sep. Purif. Methods*, **15,** 127 (1986).
Yu, Q., J. Yang, and N.-H. L. Wang, "Multicomponent Ion Exchange Chromatography for Separating Amino Acid Mixtures," *React. Polym.*, **6,** 33 (1987).

Manuscript received Dec. 21, 1989, and revision received June 25, 1990.